Conference Paper, Published Version

Durand, Noémie; Tassi, Pablo; Blanpain, Olivier; Lefebvre, Alice

Hydrodynamic modelling as a first step to assess marine dune dynamics: influence of waves

Hydrodynamic modelling as a first step to assess marine dune dynamics: influence of waves

Noémie Durand [1,3], Pablo Tassi [2,3], Olivier Blanpain [1], Alice Lefebvre [4]
noemie.durand@france-energies-marines.org, Chatou, France

[1] France Energies Marines, 525 Av. Alexis de Rochon, 29280 Plouzané, France.
[2] EDF Recherche & Développement, 6 Quai Watier, 78400 Chatou, France.
[3] Laboratoire d'Hydraulique Saint-Venant, 6 Quai Watier, 78400 Chatou, France.
[4] MARUM, University of Bremen, Leobener Str. 8, 28359 Bremen, Germany.

Abstract – **Tides, winds, and waves shape the seabed of shallow shelf seas. In sandy, energetic environments, marine dunes can develop. The size and mobility of these bed forms warrant some interest, for example related to the interactions with offshore wind farms. Yet, the morphology and dynamics of dunes are still poorly understood in open marine environments.**

A fully coupled, Reynolds-Averaged Navier-Stokes three-dimensional coastal area model is being developed for an application on the North Sea French coast (Dunkirk).

Keywords: Marine dunes, Sediment transport, Hydrodynamics, Waves, Model calibration, TOMAWAC.

I. INTRODUCTION

Marine dunes are large, flow-transverse bed forms with height of 1 m to 5 m and wavelength of the order of hundreds of metres [1]. They develop almost exclusively on sandy seabeds, in settings where bedload is the predominant mechanism of sediment transport. They are very dynamic: growing, evolving and migrating, at rates of up to tens of metres per year.

Marine dunes are widely present in shallow shelf seas, like the North Sea, where they interact with human activities. The interaction of these large-scale morphodynamic structures with offshore wind farm (OWF) elements is of particular interest. At the end of 2020, there were about 5400 offshore wind turbines, installed or under construction, in European waters alone [2].

One such wind farm project is planned offshore of Dunkirk, on the northern coast of France, close to the Belgium border. Marine dunes of all sizes coexist there with sand banks (Figure 1). A large data set has been collected in the last few years for fundamental research and in support of the OWF project. Recurrent bathymetric surveys indicate average dune migration rates of the order of 30 metres per year towards the North-East.

A numerical model is being developed that aims to reproduce the evolution of the dune field through time scales of 1 month to 5 years. Because the combined influence of currents and waves mobilise the sediments on the seabed, adequately understanding and predicting the prevailing hydrodynamic and wave conditions is a prerequisite to a correct prediction of sediment transport patterns and the dynamics of marine dunes. This paper focuses on the development and validation of a wave model based on TOMAWAC [3] against field data. The development and validation of the companion flow model is the subject of [4] and is only briefly referred to here.

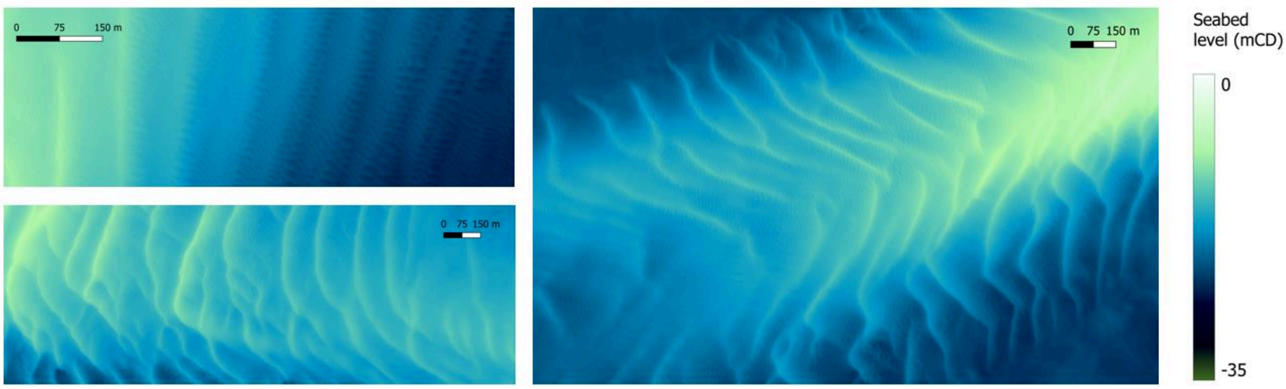

Figure 1. Example of marine dune fields, observed offshore of Dunkirk (Source of the data: Eoliennes en Mer de Dunkerque (EMD))

II. Contribution of waves to sediment transport in the study area

Water particles in a wave follow an orbital motion, which diameter corresponds to the wave height near the surface. Closer to the seabed, in intermediate and shallow water, this motion induces oscillatory currents, whose strength depends on water depth, wave height and period. Although these currents do not generate net sediment transport, they are susceptible to mobilise the sediment particles. The sediment grains are then available to be transported, for example by the tidal currents.

Owing to the location and depth of the study area, it is anticipated that wave effects reach the seabed during storm events. One of the first steps was, therefore, to check this assumption, to determine whether the modelling should include wave contributions.

The grain bed shear-stresses τ_0 induced by currents and waves were estimated separately, from observations available at a location within the proposed wind farm, in ca. 16 m water depth, between May 2021 and February 2022 (Source of the data: EMD). The shear-stresses generated by currents alone were computed from the water density $\rho = 1027$ kg/m^3, the depth-averaged current speed U, and the drag coefficient C_D assuming a power law velocity profile [5]:

$$(\tau_0)_{\text{currents}} = \rho\, C_D\, U^2. \quad (1)$$

Those generated by waves alone were computed using an approximation that gives the root-mean-square orbital velocity for a JONSWAP spectrum U_{rms} [6], and the wave friction factor f_w defined in [5]:

$$(\tau_0)_{\text{waves}} = \rho\, f_w\, U_{rms}^2. \quad (2)$$

These calculations are simplifying but deemed adequate as a first approximation to assess the role of waves in the sediment transport, in comparison to currents. The results of this analysis are presented in Figures 2 and 3 for a 4-day period in June and in February, respectively. For completeness, the threshold of motion is indicated on these figures as a dashed black line. It was computed for a well sorted sediment with median grain diameter d_{50} = 345 µm, which is representative of the average granulometry in the study area.

The quarter-diurnal variations in tide-induced bed shear-stress are apparent in Figures 2 and 3 (as are the variations through the spring-neap cycle – not shown). In the absence of wind, the magnitude of the peak shear-stress associated with maximum neap currents is of the order of 0.4 N/m^2; 0.8 N/m^2 for spring currents. It can reach 1.5 N/m^2 during stormy periods.

Semidiurnal variations in the wave-induced bed shear-stress are also evident in Figures 2 and 3 in response to the tidal modulations (water level fluctuations and Doppler shifting). In comparison, wave-induced bed shear-stresses are negligible in the summer period (Figure 2), barely reaching 0.1 N/m^2. They are, however, comparable in magnitude to the current-induced bed shear-stresses during the winter period (Figure 3), even at this relatively deep location, with a peak value of 1.3 N/m^2. When considered in relation to the critical shear-stress for onset of movement, it is clear that sediment grains are likely to be mobilised by waves during these times.

It is noteworthy that current reversal does not occur at high / low water in the study area, but is delayed by two to three hours, meaning that low water nearly coincides with peak ebb currents (trending South-West). This is also when wave-induced bed shear-stresses peak. It is, therefore, expected that the additional friction generated by the waves will have an important dynamic and morphogenic effect and it seems essential to take waves into account in the modelling as a result.

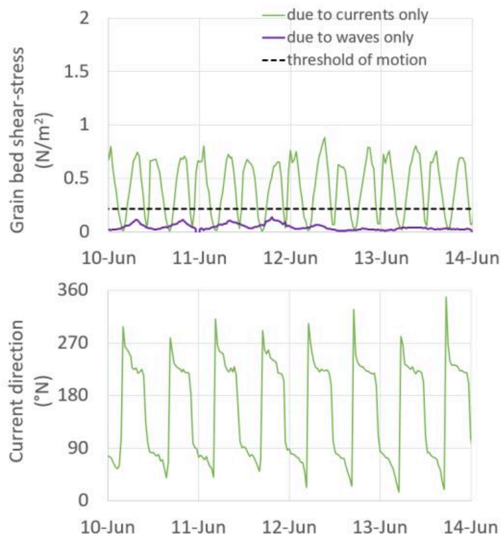

Figure 2. Grain bed shear-stresses estimated from EMD current and wave data observed in the summer of 2021

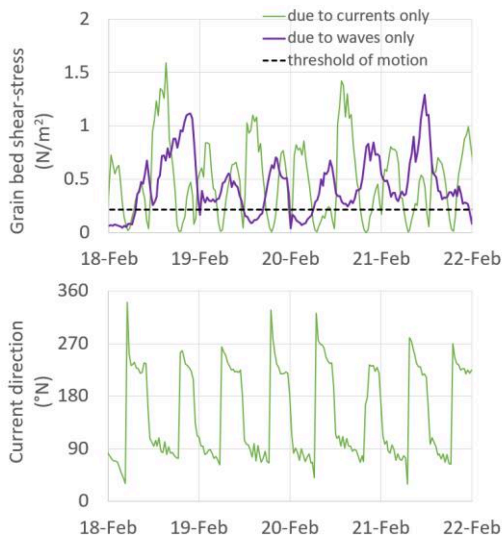

Figure 3. Grain bed shear-stresses estimated from EMD current and wave data observed in the winter of 2022

III. Dunkirk approaches wave model setup

The open TELEMAC system is applied to Dunkirk and its approaches to investigate the dynamics of marine dunes in a shallow shelf sea environment. To that effect, hydrodynamic, wave and morphodynamic models are being set up, independently calibrated and validated, then internally coupled. The following presents the setup of the TOMAWAC wave model. The development and validation of the companion flow model is the subject of [4].

A. Model extent and mesh resolution

The model extends for approximately 80 km along the coast, from the port of Calais in the West to Ostend in Belgium in the East. Its offshore extent varies between 15 km in the Dover Strait and 75 km in the East. The model full extent is shown in colour in Figure 4 superimposed on HOMOMIM bathymetry [7] (grey shades) and OpenTopoMap [8] data.

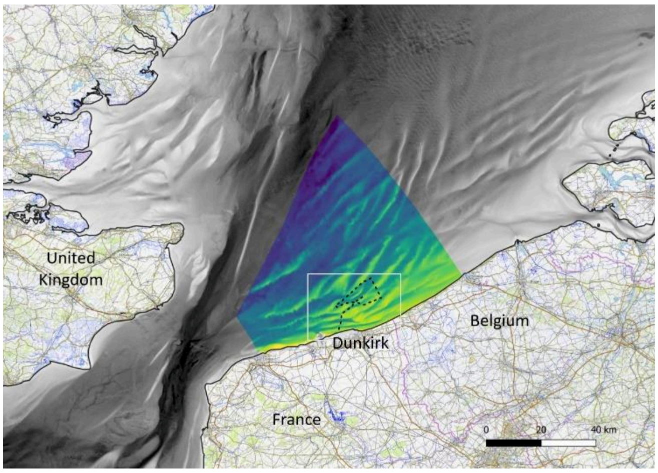

Figure 4. Location map showing the full model extent (in colour) and the proposed offshore wind farm footprint (dashed line) (Source of the background data: [7] and [8])

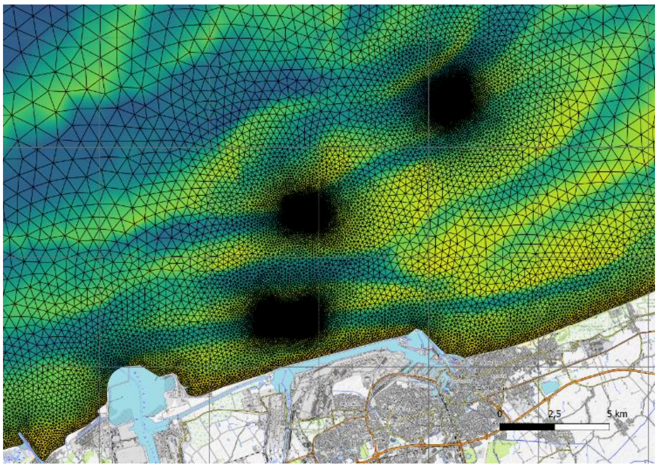

Figure 5. Close-up view of the mesh resolution around Dunkirk, showing increased resolution (10 m) in the three bathymetry tiles (Source of the background data: [8])

Given the extent of the model area, a triangular finite element mesh with spatially varying resolution was used. The size of the elements varied gradually from 1400 m away from the area of interest down to 100 m at the shoreline. A finer resolution of ca. 10 m was used to represent the three tiles where recurrent bathymetric surveys had been conducted and where we aim to reproduce the evolution of the dune field. This element size is deemed adequate for the purposes of calibration and validation of the hydrodynamic and wave models; further mesh refinements may be necessary for the morphodynamic modelling.

Overall, the model area comprises approximately 60 k nodes and 117 k elements. A close-up view of the variable mesh resolution is shown in Figure 5 for the area identified by a white rectangle in Figure 4.

B. Seabed map

Digital elevation models of the seabed throughout the model area are being constructed that are relevant to different time periods. This is done by combining a range of data sources, where superior data take precedence over data of lesser quality / resolution. Best judgement is being used to integrate data pertaining to different time periods as seamlessly as possible in this highly dynamic environment.

A preliminary seabed map was, however, used for the simulations presented in this paper, which is based solely on the HOMONIM data set [7] as a first approximation. This seabed map is illustrated in Figure 4.

C. Wave forcing

TOMAWAC is driven by wave conditions imposed along the open boundaries. In this study offshore wave data obtained from two different sources were compared: integrated sea states from the ECMWF ERA5 reanalysis data set, and spectral sea states from the ANEMOC-3 hindcast database.

ERA5 ([9] and [10]) is a climate reanalysis data set, generated using Copernicus Climate Change Service (C3S) information. The name refers to the fifth major global reanalysis produced by the European Centre for Medium-Range Weather Forecasts (ECMWF). It provides high quality medium-resolution estimates of atmospheric and surface wave parameters, with a horizontal resolution of 0.25° and 0.50° respectively. Data are archived hourly and were obtained at point 2.0°E 51.7°N.

ANEMOC-3 ([11] and [12]) is the third revision of the ANEMOC database originally developed by EDF R&D and Cerema to hindcast sea states around the French coast (ANEMOC stands for Atlas Numérique d'Etats de Mer Océanique et Côtier). The database covers the Atlantic, the English Channel and North Sea French coast, down to 0.01° horizontal resolution. ANEMOC-3 is developed based on the TOMAWAC 3rd generation wave model [3], where tidal effects are accounted for through water level and current maps predicted using a TELEMAC-2D hydrodynamic model of the same area. The ANEMOC-3 database has recently been updated and extended to include 2021 [12].

Time-varying wave spectra were obtained at 56 locations along the open boundaries of the wave model. The spectra are discretised with 32 frequencies and 36 directions. The use of spectral data is preferred over integrated sea states, in that it reduces the loss of information at the interface between the hindcast database and our local wave model.

The suitability of these two data sources was assessed by comparing them to wave measurements available at Westhinder from a directional wave rider buoy located at 2°26'08" E 51°22'51" N (Source of the data: VLIZ). The buoy was deployed in January 1997 in approximately 23 m water depth. The recorded parameters include wave height, average wave period, and direction of the swell and wind-sea components. The wave climate is depicted in Figure 6 as a wave rose.

At Westhinder buoy, waves are predominantly from the West-South-West, with some significant events from the North-West through to the North-East. 56% of the waves are under 1 m. The highest wave on record is 5.7 m from the South-West; the second highest 5.6 m from the North-West.

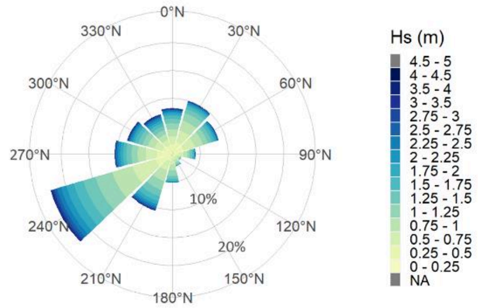

Figure 6. Wave climate at Westhinder buoy (Source of the data: VLIZ)

Wave heights extracted from the ANEMOC-3 database at Westhinder buoy for 2021 were compared to those observed during the same period. Considering a whole year removes any seasonal bias. The result of the comparison on a direct time for time basis is shown as a scatter plot in Figure 7. ANEMOC-3 appears to under-estimate wave heights above 1.5 m at Westhinder, by approximately 7%. The same analysis was performed for mean wave period. It indicated that mean periods were under-predicted by 0.5 s on average. This agreement was deemed satisfactory enough that no correction was applied to the ANEMOC-3 wave spectra in the first instance, before they were used as input to the wave model.

The resolution of the ERA5 data set (approximately 35 km East-West by 56 km North-South for ocean wave data) did not allow a similar comparison to be drawn. The wave heights and periods recorded at Westhinder buoy were bounded by the heights and periods extracted from ERA5 data points on either side of the buoy. Still, the use of ERA5 integrated sea states was carried through in the simulations, as a sensitivity to offshore boundary conditions.

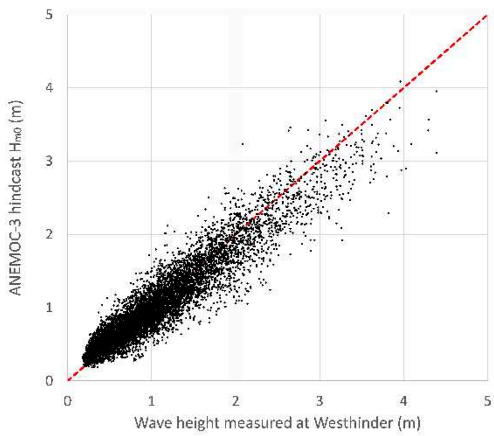

Figure 7. ANEMOC-3 hindcast wave data compared to wave measurements at Westhinder buoy for 2021

D. *Meteorological forcing*

In addition to wave forcing at the open boundaries, TOMAWAC is also driven by wind forcing processes, which account for local wave generation due to winds. Two sources of offshore wind data were considered and compared to in-situ observations: the ERA5 reanalysis data set, and the AROME database.

AROME [13] is an operational forecast from Météo-France, designed specifically to improve the short-term forecasting of dangerous phenomena such as heavy rains, violent storms, fog or urban heat pockets. The initial model conditions are derived from assimilation of radar network data (precipitation and Doppler winds), with an hourly frequency. The model predictions are available up to 42 hours ahead, at a high resolution of 0.025°. Data are archived hourly and were obtained from the 30-hour forecast over the whole model area such that spatially varying, as well as temporally varying, wind fields could be applied.

Long-term wind measurements are available at Westhinder from an instrumented pile located at 2°26’16" E 51°23’18" N (Source of the data: VLIZ). Water level, wind and pressure data are recorded since January 1997. The wind climate is presented in Figure 8. Winds come largely from the South-West and the Channel.

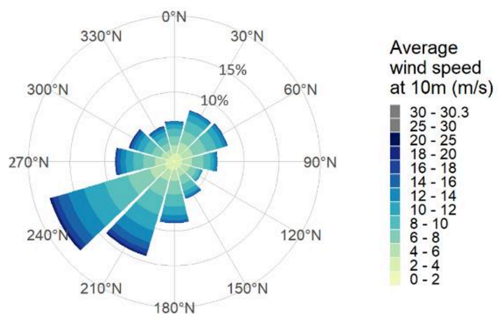

Figure 8. Wind climate at Westhinder pile (Source of the data: VLIZ)

Both sources of offshore wind were compared against these open sea observations for 2021. The AROME winds agree more closely with the measurements (as shown in Figure 9) than the ERA5 hindcast winds did, and so it was decided to use AROME in our application.

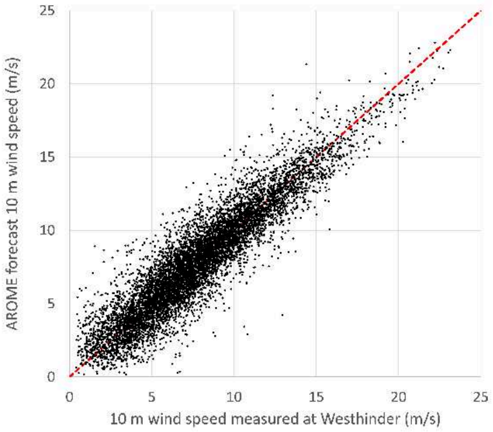

Figure 9. AROME forecast wind data compared to open sea wind measurements at Westhinder pile for 2021

Local wave generation due to winds is accounted for in the model using the WAM cycle 3 formulation, and linear wave growth as in Cavaleri and Malanotte-Rizzoli (1981).

E. Tidal forcing

In shallow shelf seas, tidal effects also play a role on wave propagation and transformation. The currents cause refraction of the waves, Doppler shifting, and in some cases (strong opposing currents) blocking of the waves. In simple environments, opposing currents are expected to steepen the waves, enhancing their height and reducing their wavelength, whilst following currents would dampen wave heights and increase wavelengths.

These effects were considered in the wave model by way of spatially and temporally varying maps of water levels and currents, obtained from a calibrated hydrodynamic TELEMAC model of the same area. This model is described in some detail in [4]. It is driven by harmonic constituents (34) extracted from the FES2014 database [14] produced by Noveltis, Legos and CLS.

The wave model results were found to be quite sensitive to the choice of formulation used to account for the tidal modulations. 'DISSIPATION BY STRONG CURRENT' = 0 seemed to exaggerate the effect of the currents on wave periods and directions. Reasonable results were had when a dissipative term was added as in Van der Westhuysen (2012) (option 2), provided that the dissipation coefficient was tuned. The best results were obtained when the spectra were limited using a Phillips (1977) shape (option 1).

IV. PRELIMINARY CALIBRATION

A. Wave data sources

Wave data were collected in recent years in the study area for fundamental research and in support of the Dunkirk OWF project (Sites 1 to 7 in Figure 10). A range of integrated wave parameters, of which significant wave height H_{m0}, mean wave period T_{m02}, peak wave period T_p, and mean direction, are available:

- in September 2016 at Sites 1 and 2 (Source of the data: SHOM),
- between October 2020 and April 2021 at Site 6 (Source of the data: EMD),
- between May 2021 and February 2022 at Site 7 (Source of the data: EMD).

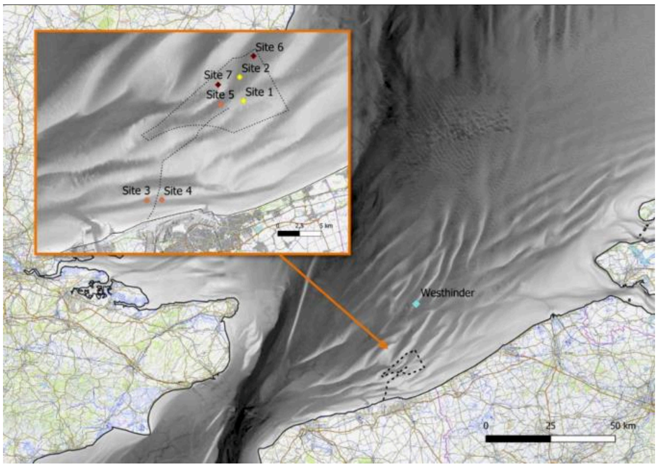

Figure 10. Map showing the location of wave observations in relation to the OWF footprint (Source of the background data: [7] and [8])

Wave data collected at Sites 3 to 5 for approximately 40 days in the Spring of 2021 (Source of the data: FEM) were obtained in raw format and have not been analysed to date.

Wave height and average wave period (taken to be significant wave height $H_{1/3}$ and zero-crossing wave period T_z) are recorded at Westhinder buoy (Figure 10) since 1997 at 30-minute intervals, with relatively minor interruptions in the records. These observed data, albeit further from our area of interest, were also used to assess the performance of the wave model in transforming the offshore waves to the study area.

B. Model comparisons with in-situ data

Given the location of the study area, it is important that the wave model be able to predict accurately the tidal modulations (i.e., the increase or reduction in wave height and period, as well as the change in direction, caused by the current conditions) throughout the tidal cycle. If it can be shown that the model results agree with the in-situ measurements, then it gives confidence in the wave predictions for normal and extreme events.

Two energetic periods were simulated, one in the Autumn of 2016 and the other in the Spring of 2021, for which model predictions were compared to the mooring data presented earlier in the OWF area and at Westhinder buoy. It is reminded that, at this preliminary stage, the most recent bathymetric data have not been incorporated in the current version of the wave model and the model seabed map is a closer representation of the 2016 conditions than it is of the 2021 conditions. As such closer agreement can be expected against data observed in 2016.

The comparisons shown in Figures 11 and 12 are favourable in terms of significant wave height, mean wave period and mean wave direction (all of which have an impact on sediment transport). There seems to be a tendency to under-predict the storm waves during the first period (Figure 11). The tidal effects are apparent in these figures, in particular Doppler shifting and refraction by the currents, and are reasonably well reproduced by the wave model. Some differences are observed. They could be attributed to deficiencies in the offshore wave data, the wave model, inaccuracies in the measured values, or possibly a combination of the three.

To quantify these differences between predictions and measurements, Root Mean Square Errors (RMSE) were computed. The results of this analysis are summarised in Table I for the entire simulation period. Values in brackets were computed based on storm events only. It is expected that agreement at Westhinder could be further improved should the mesh be more finely resolved there (the mesh size is currently of the order of 1 km).

Table I Performance of the wave model against observed data

	RMSE on H_{m0}	**RMSE on T_{m02}**	**RMSE on mean direction**
	September 1 to October 10, 2016		
Site 1	0.13 m (0.20 m)	0.5 s (0.6 s)	39° (15°)
Site 2	0.15 m (0.18 m)	0.4 s (0.4 s)	55° (30°)
Westhinder	0.18 m (0.22 m)	0.6 s (0.5 s)	--
	May 15 to May 30, 2021		
Site 7	0.20 m (0.18 m)	0.5 s (0.5 s)	20° (9°)
Westhinder	0.22 m (0.29 m)	0.5 s (0.5 s)	--

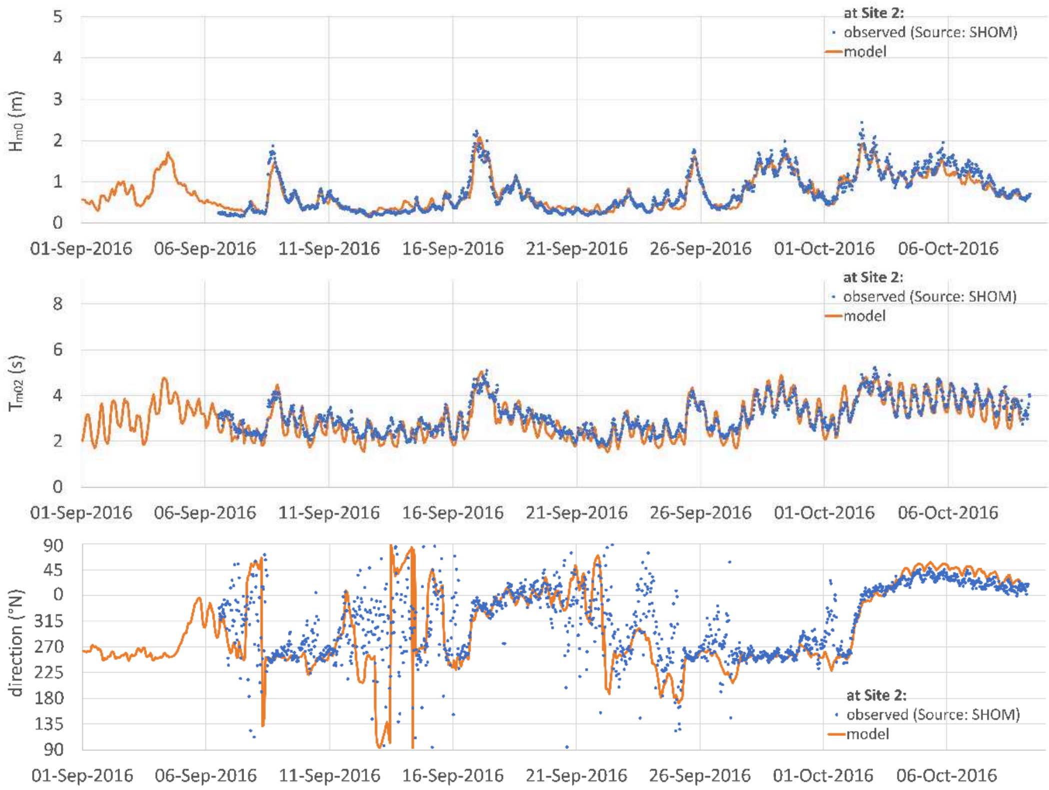

Figure 11. Comparison of model predictions against observed significant wave height H_{m0} (top), mean wave period T_{m02} (centre), and mean wave direction (bottom) at Site 2 between September 1 and October 10, 2016

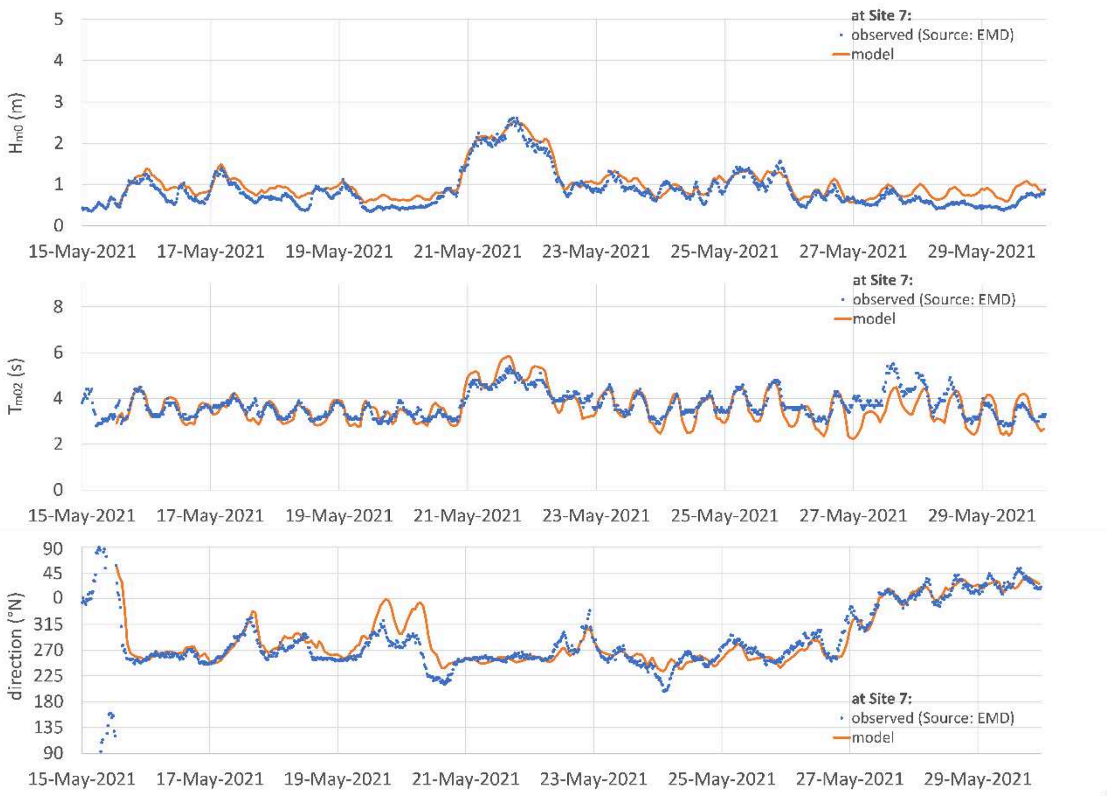

Figure 12. Comparison of model predictions against observed significant wave height H_{m0} (top), mean wave period T_{m02} (centre), and mean wave direction (bottom) at Site 7 between May 15 and May 30, 2021

It is noteworthy that, despite the relatively coarse resolution of the ERA5 data set, which meant that spatially uniform wave boundary conditions had to be applied (conditional to wave incidence), the transformation of the waves as they travel in shallow waters to the moorings was well modelled. Comparable agreement with measurements was obtained with that approach. The use of ANEMOC-3 spectral input is expected to be superior when mixed seas prevail, where the direction of the background swell and that of the winds do not coincide, or when remnants of old storm events are still present. Few such events were, however, initially observed.

With the current model configuration, it takes just over 1.5 hours to simulate one day on one compute node (two Intel® Xeon® Platinum 8260 24-core 2.40 GHz processors = 48 cores). The run times were marginally shorter when uniform boundary conditions were applied from integrated sea states.

V. Conclusion and future work

It has been shown that waves are expected to play a role in sediment transport in the study area. Further analysis would indicate to which extent. Given the large computational times of the wave model, there may be a need to optimize the exchange of information between the hydrodynamic, wave and sediment transport models for the morphodynamic simulations. For example, it could be appropriate to relax the coupling period of the wave model when wave activity is not expected to contribute much to sediment transport (to be determined).

Overall, the comparisons presented in this paper indicate that the wave model provides a good prediction of wave conditions in the study area under a range of tidal currents and offshore wave and wind conditions. Importantly the ability of the model to simulate tidal modulations has been demonstrated. This is expected to be critical moving forward to morphodynamic simulations.

Next, the sediment transport and bed evolution processes will be modelled by means of a 3-way coupling between the TELEMAC-3D, TOMAWAC and GAIA modules. Once satisfactory agreement is reached against observed in-situ bathymetry survey data, this comprehensive coastal area model will be used as a research tool to better understand marine dune dynamics in the Dunkirk area and their interactions with OWF elements.

Acknowledgements

This work was initiated by France Energies Marines, with support from the French government, under the "Investissements d'Avenir" programme managed by the French National Research Agency ANR. The authors would like to thank the partners of the MODULLES project for providing site-specific data and giving permission to publish this work.

REFERENCES

[1] G. M. Ashley, "Classification of large-scale subaqueous bedforms: A new look at an old problem". Journal of Sedimentary Petrology, Vol. 60, No. 1, 1990, pp 160-172. https://doi.org/10.2110/jsr.60.160

[2] The Crown Estate, "Offshore wind operational report 2020". Technical report, 2020

[3] M. Benoit, F. Marcos, F. Becq, "Development of a third generation shallow-water wave model with unstructured spatial meshing". In Proc. 25th Int. Conf. on Coastal Eng. (ICCE'1996), 2-6 September 1996, Orlando, pp 465-478. https://doi.org/10.9753/icce.v25.%25p

[4] N. Durand, P. Tassi, O. Blanpain, A. Lefebvre, "Towards numerical modelling of marine dunes in a shallow shelf sea". In Actes des XVIIèmes Journées Nationales Génie Côtier-Génie Civil, Chatou, France, 2022. in press

[5] R. Soulsby, "Dynamics of marine sands". Thomas Telford Publishing, 1997. https://doi.org/10.1680/doms.25844

[6] R. Soulsby, "Simplified calculation of wave orbital velocities". HR Wallingford Technical Report TR 155, 2006

[7] SHOM, MNT bathymétrique de façade atlantique (projet HOMONIM). 2015. http://dx.doi.org/10.17183/MNT_ATL100m_HOMONIM_WGS84

[8] https://opentopomap.org/

[9] H. Hersbach and D. Dee, "ERA5 reanalysis is in production". ECMWF Newsletter Number 147 - Spring 2016. Published in April 2016

[10] ERA5, https://doi.org/10.24381/cds.adbb2d47

[11] C. Raoult, A. Joly, M. Andreevsky, and A. Joly-Laugel, "ANEMOC-3: Improving the ANEMOC-2 Sea state database by adding tide effects". In Actes des 16èmes Journées de l'Hydrodynamique, 27-29 Novembre 2018, Marseille, France

[12] M. Teles, M. Weiss and M. Benoit, "Assessment of the ANEMOC-3 sea state hindcast database for modelling a series of energetic winter storms along the French coast". In Actes des XVIIèmes Journées Nationales Génie Côtier-Génie Civil, Chatou, France, 2022. in press

[13] F. Boutier, "Arome, avenir de la prévision régionale". La Météorologie, No. 58, 2007, pp 12-20. https://doi.org/10.4267/2042/18203

[14] FES2014, https://www.aviso.altimetry.fr/